ADAS

Atomic Data and Analysis Structure

University of Strathclyde Glasgow

Determination of divertor temperature and density using N II line ratios

Stuart Henderson[1]

in collaboration with M. Carr[2], M. O'Mullane[1], F. Reimold[3], M. Bernert[4] & the MST1 team

[1] Department of Physics, University of Strathclyde, Glasgow G4 0NG, UK

[2] EURATOM/CCFE Fusion Association, Culham Science Centre, Abingdon, Oxfordshire, OX143DB

[3] Forschungszentrum Juelich GmbH, Trilateral Euregio Cluster, 52425 Juelich, Germany

[4] Max-Planck-Institute for Plasma Physics, D-85748 Garching, Germany

20th ADAS Workshop, NFRI Gunsan, Korea, 29-30th September 2016

This work has been carried out within the framework of the EUROfusion Consortium and has received funding from the Euratom research and training programme 2014-2018 under grant agreement No 633053. The views and opinions expressed herein do not necessarily reflect those of the European Commission.

Talk Overview

1) **Introduce spectroscopic techniques used in analysis**

   – *Balmer and impurity spectroscopy*

2) **Illustrate AUG divertor setup**

   – *Geometric layout*
   – *SOL Plasma Simulation*

3) **Atomic modelling of N II emission**

   – *Line intensities and ratios*
   – *ADAS feature generation (AFG)*
   – *Framework for Feature Synthesis (FFS)*

4) **Temporal behaviour of fitted parameters**

   – n_{N1+}, T_e, & n_e

Introduction – Balmer spectroscopy

Balmer series emission can provide valuable information about the divertor plasma conditions

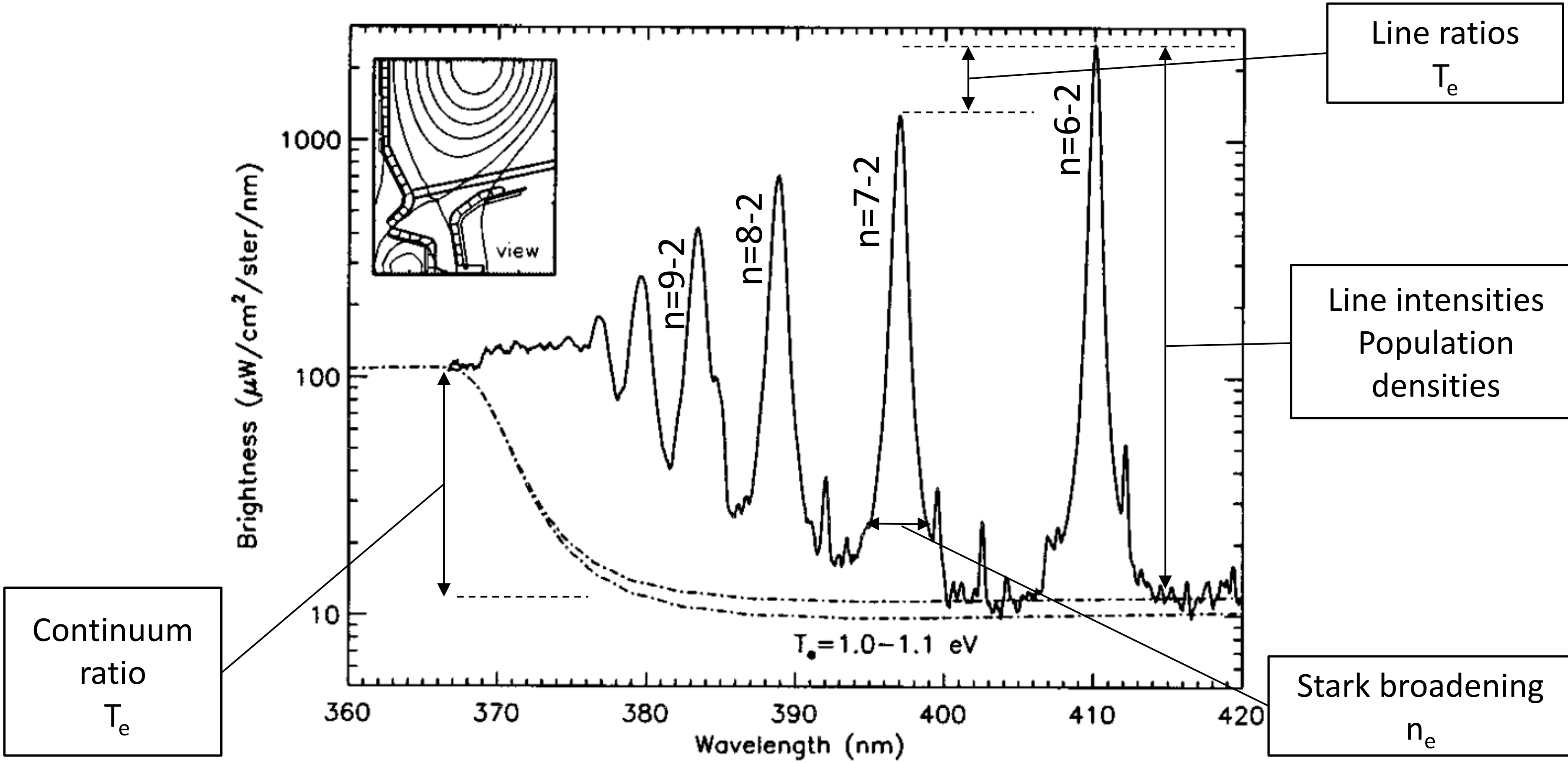

Figure 1: J.L. Terry et al. PoP **5**, 1759 (1998)

Introduction – Balmer spectroscopy

A narrow spectral range is used on AUG to measure the broadening of the H_δ and H_ε lines

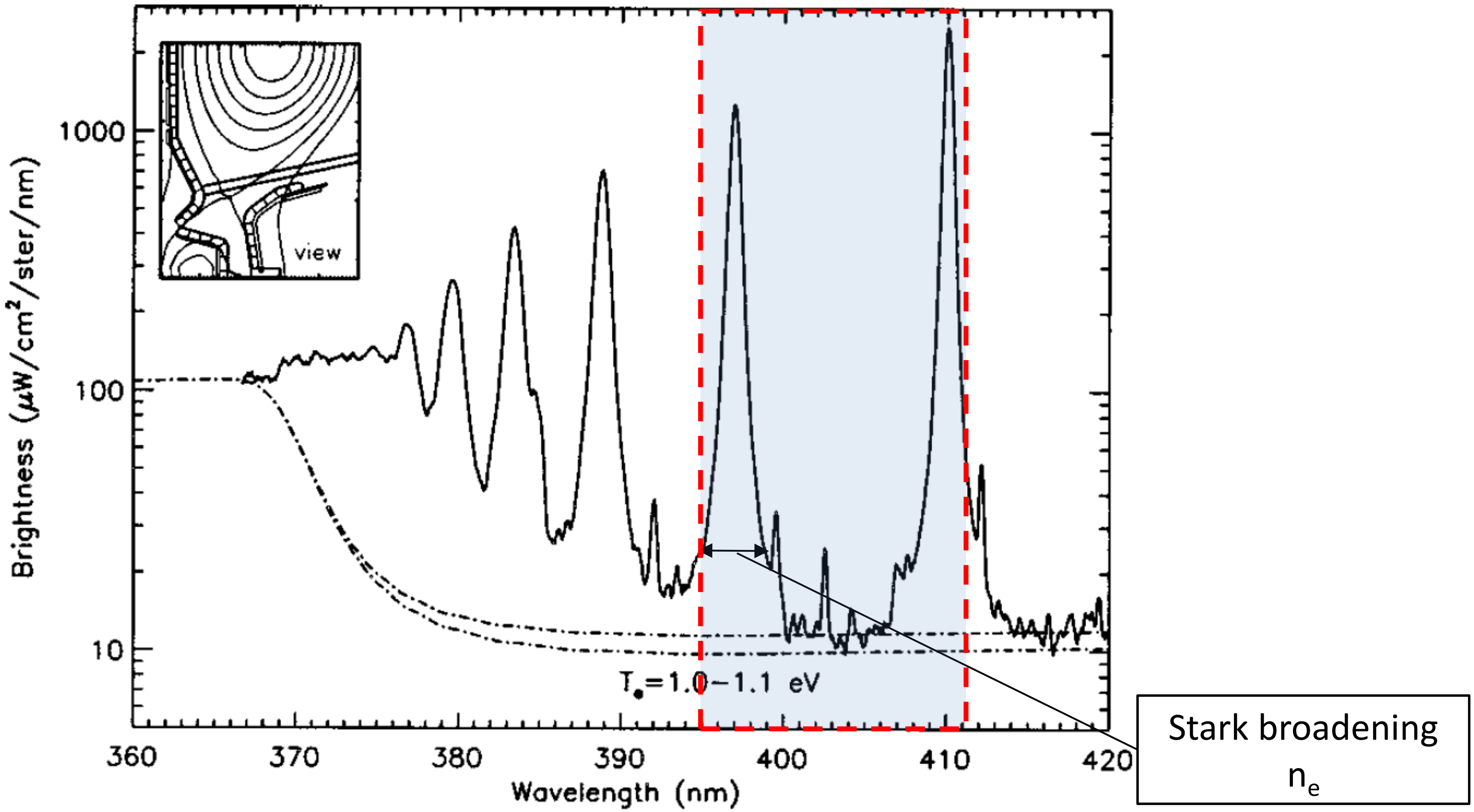

Figure 1: J.L. Terry et al. PoP **5**, 1759 (1998)

Introduction – Impurity spectroscopy

A number of impurity lines (N II, N III, N IV, He I, & W I) also emit within this narrow spectral range

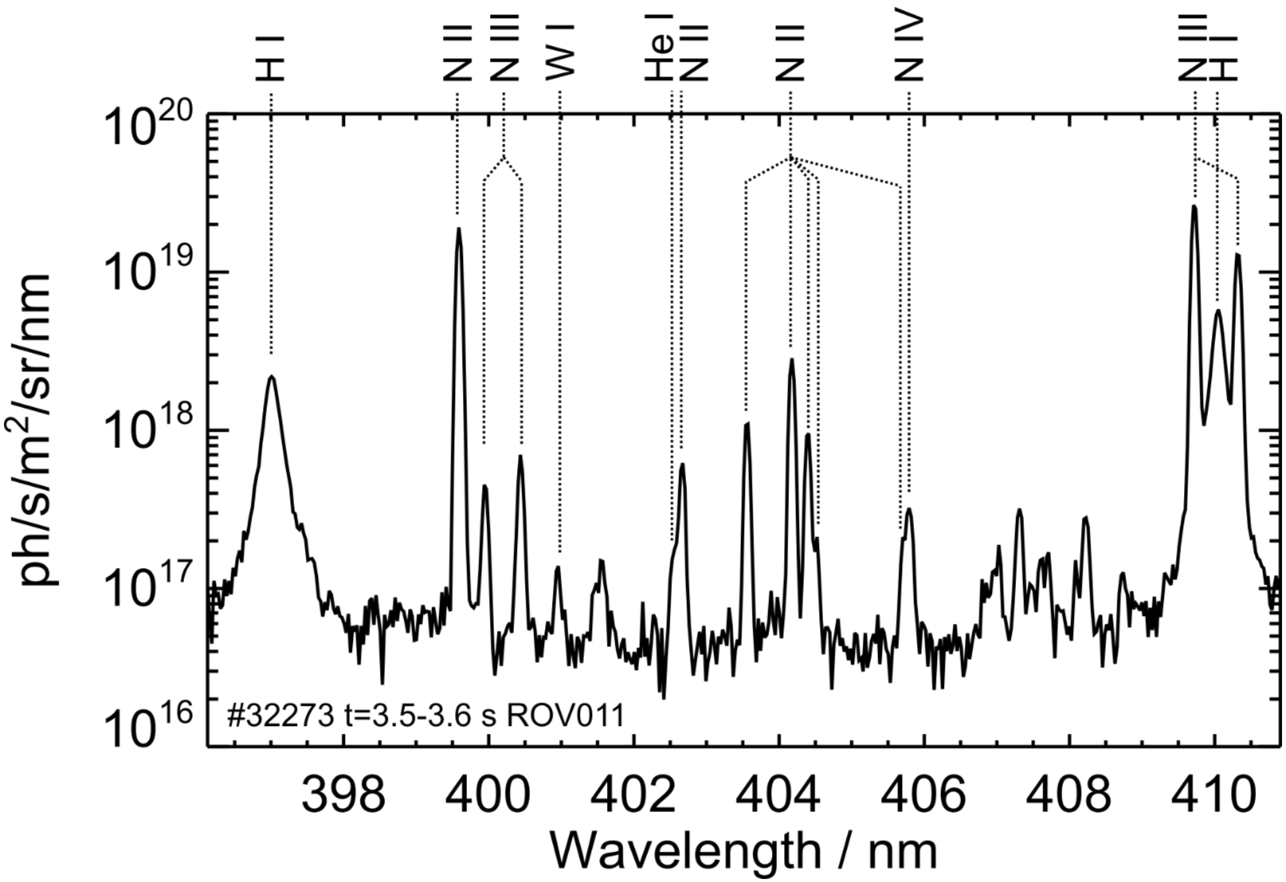

Figure 2: Spectra measured along sightline ROV011 during AUG discharge #32273

Introduction – Temperature range

The ratio of lines emanating from N II, N III, & N IV provide a measurement of n_e in hotter regions of the divertor plasma (T_e < 20 eV) in comparison to Balmer spectroscopy

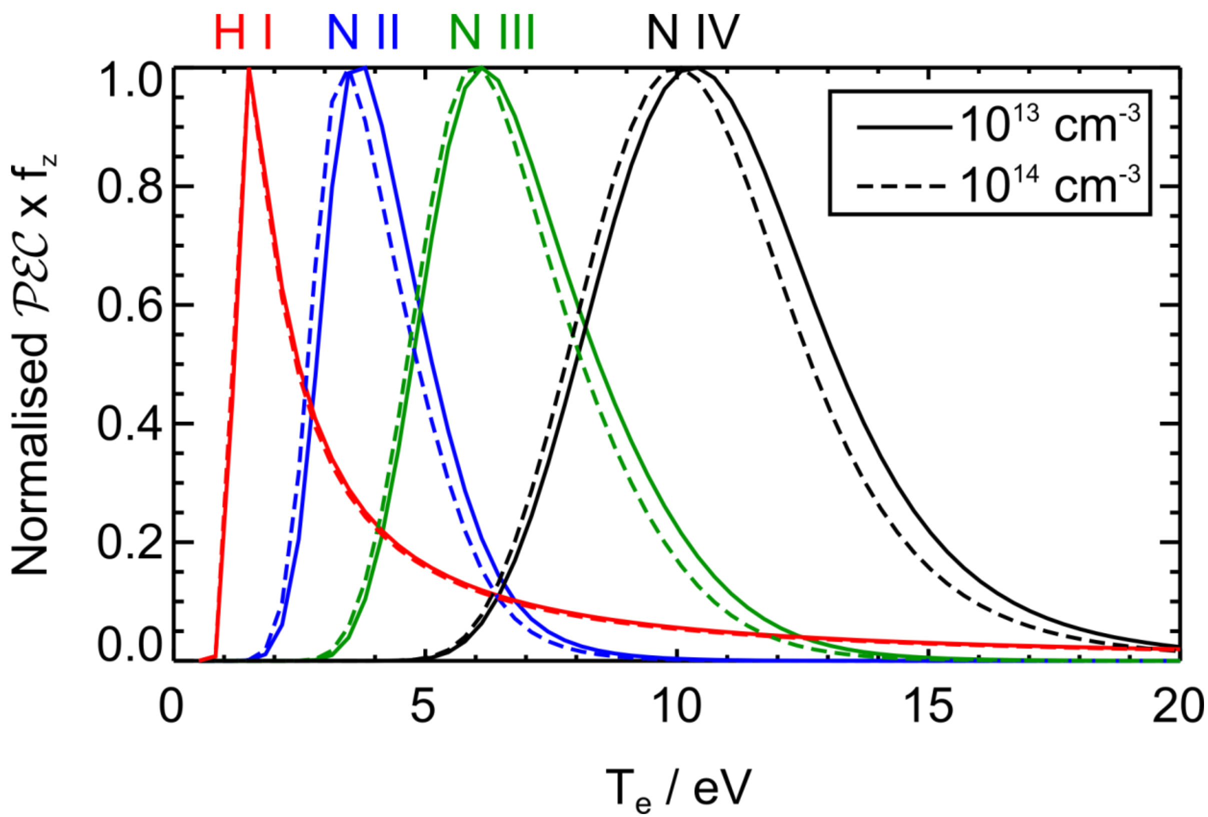

Figure 3: PECs and ionisation balance calculated using ADAS 96 data

AUG experimental setup

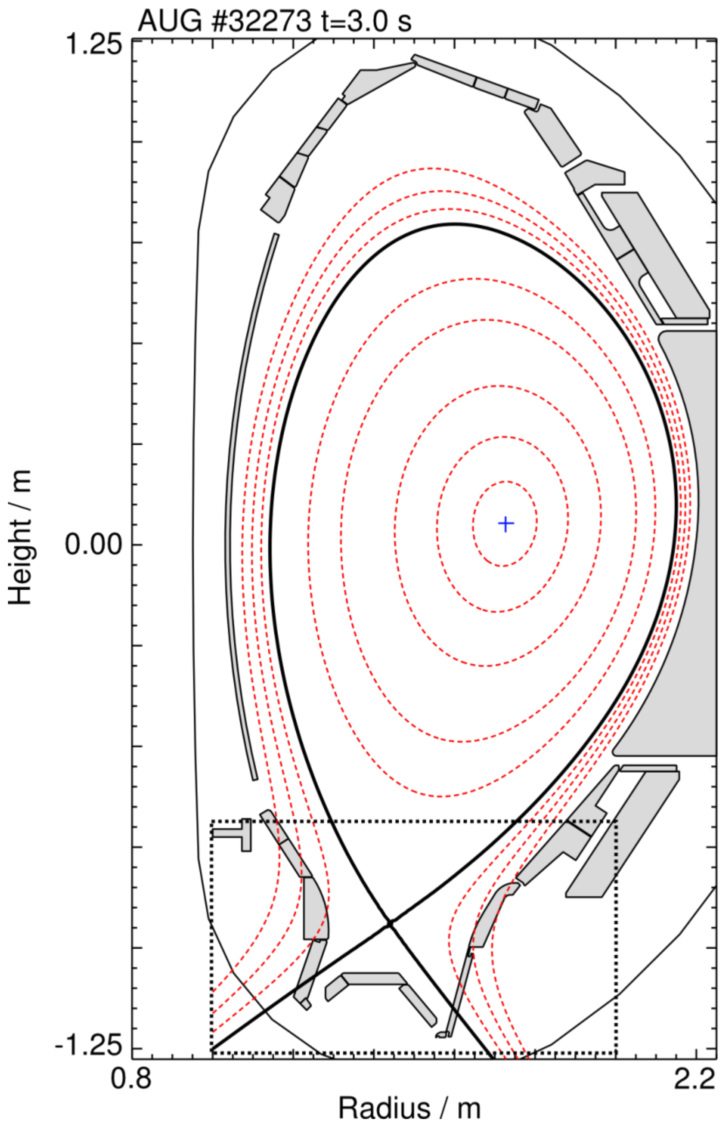

Divertor visible spectroscopy

- 396 nm < λ < 411 nm
- Instrument function: 0.08 nm
- Integration time: 2.5 ms

Sightlines

ROV009
ROV011
ROV013

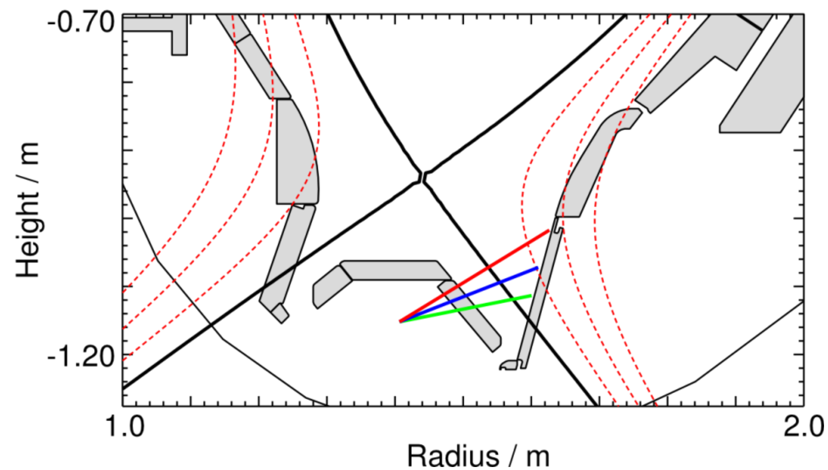

AUG experimental setup

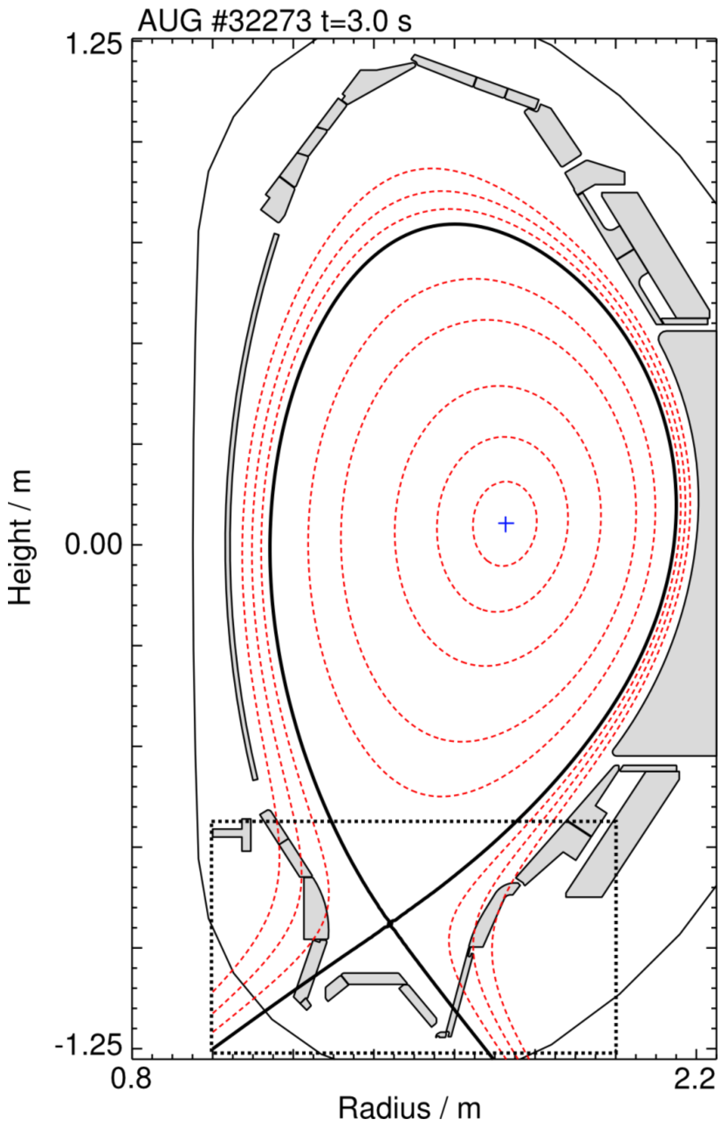

Divertor visible spectroscopy

- 396 nm < λ < 411 nm
- Instrument function: 0.08 nm
- Integration time: 2.5 ms

Sightlines

ROV009
ROV011
ROV013

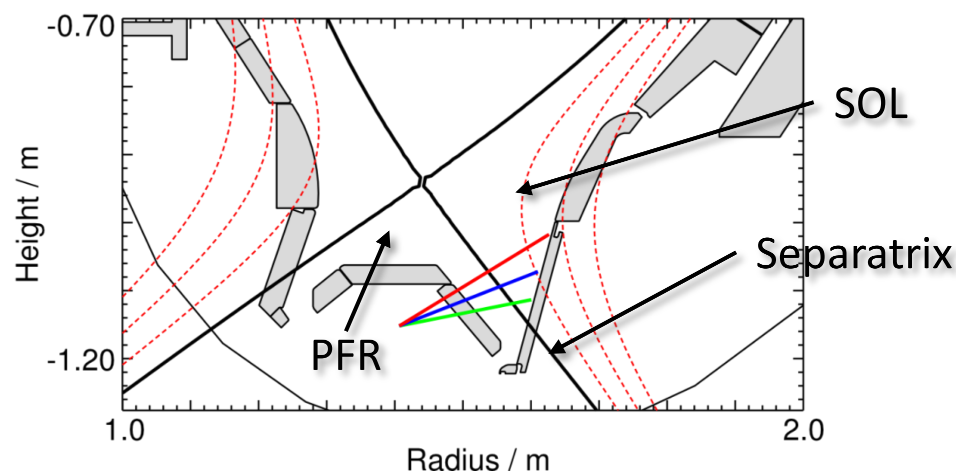

SOL Plasma Simulation

- SOLPS simulation of T_e and n_e
  - T_e in SOL too high (coupled with low n_e) for low charge nitrogen emission
  - N II, N III, & N IV emit locally in the PFR of the outer divertor leg

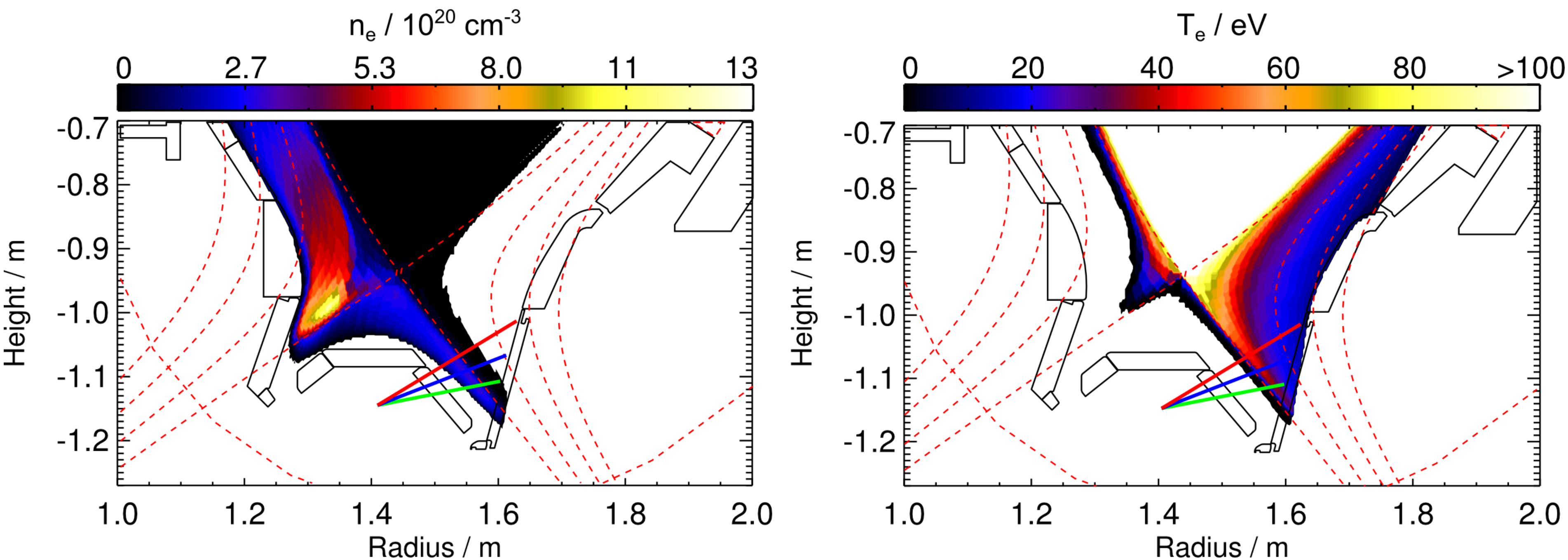

Figure 4: SOLPS simulation provided by F. Reimold

SOL Plasma Simulation

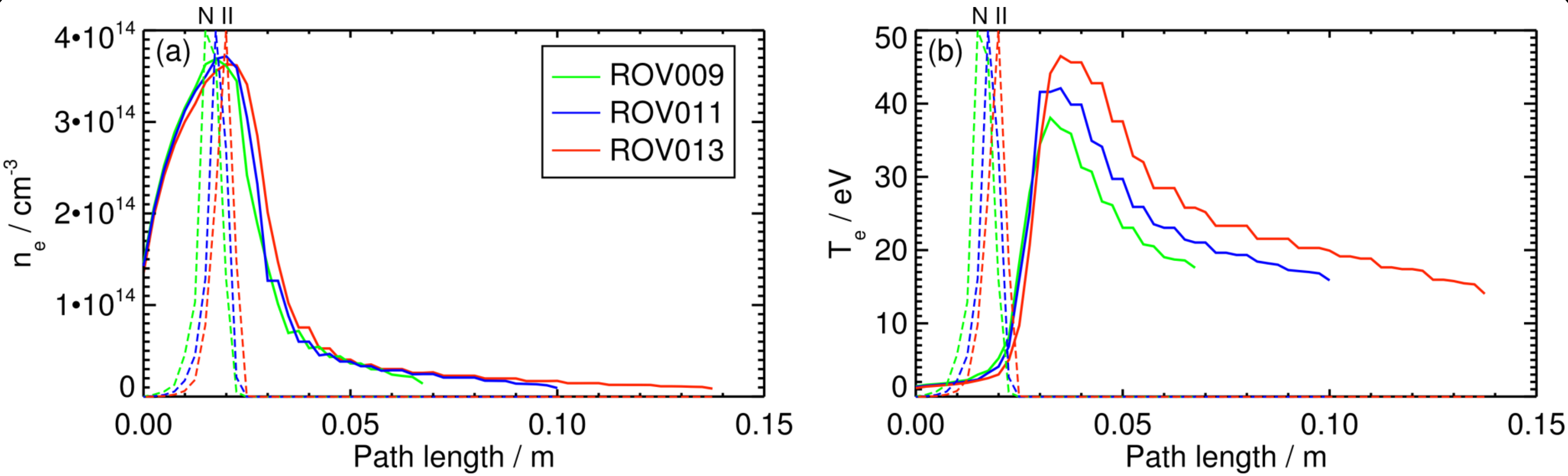

Figure 5: Sightline profiles of (a) n_e and (b) T_e as a function of the path length. Normalised N II emission is shown by the dashed lines to indicate the emitting regions.

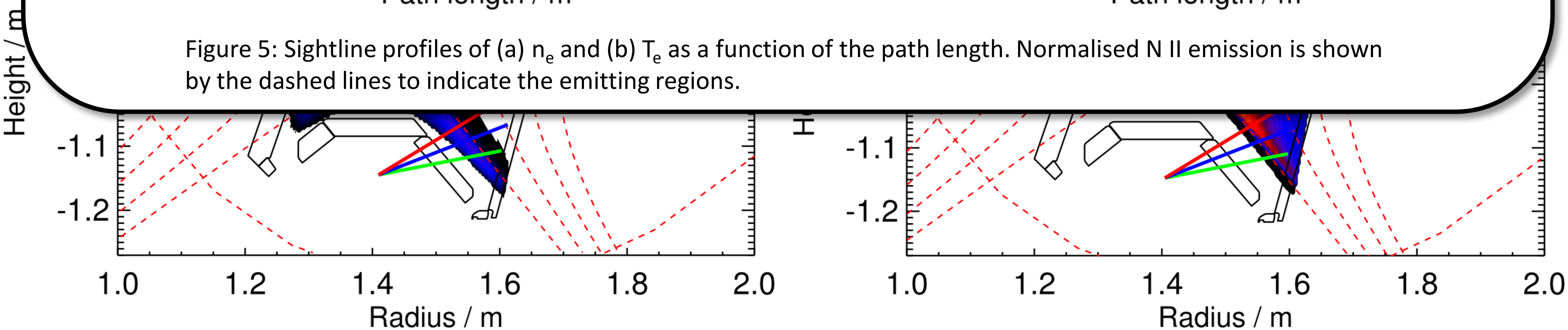

Figure 4: SOLPS simulation provided by F. Reimold

Nitrogen lines in the near UV – visible (term resolved)

(1) N II at λ ~ 344 nm: 2s2 2p 3p $^1S \rightarrow$ 2s2 2p 3s ^1P

(2) N IV at λ ~ 348 nm: 1s2 2s 3p $^3P \rightarrow$ 1s2 2s 3s ^3S

(3) N III at λ ~ 377 nm: 2s 2p 3p $^4S \rightarrow$ 2s 2p 3s ^4P

(4) N II at λ ~ 383 nm: 2s2 2p 4s $^3P \rightarrow$ 2s2 2p 3p ^3P

(5) N II at λ ~ 395 nm: 2s2 2p 3p $^1D \rightarrow$ 2s2 2p 3s ^3P

(6) N II at λ ~ 399.5 nm: 2s2 2p 3p $^1D \rightarrow$ 2s2 2p 3s ^1P

(7) N III at λ ~ 400 nm: 2s2 5f $^2F \rightarrow$ 2s2 4d ^2D

(8) N II at λ ~ 402.5 nm: 2s2 2p 4f $^1G \rightarrow$ 2s2 2p 3d ^3F

(9) N II at λ ~ 404.0 nm: 2s2 2p 4f $^3G \rightarrow$ 2s2 2p 3d ^3F

(10) N IV at λ ~ 406 nm: 1s2 2s 3d $^1D \rightarrow$ 1s2 2s 3p ^1P

(11) N III at λ ~ 409 nm: 2s2 3p $^2P \rightarrow$ 2s2 3s ^2S

(12) N II at λ ~ 413 nm: 2s 2p2 3p $^5S \rightarrow$ 2s 2p2 3s ^5P

(13) N II at λ ~ 422 nm: 2s2 2p 4s $^1P \rightarrow$ 2s2 2p 3p ^1D

(14) N III at λ ~ 420 nm: 2s 2p 3p $^2D \rightarrow$ 2s 2p 3s ^2P

- This analysis focuses on **three** N II lines

– λ ~ **399.5 nm**: 2s2 2p 3p ^1D - 2s2 2p 3s ^1P

– λ ~ **402.5 nm**: 2s2 2p 4f ^1G - 2s2 2p 3d ^3F

– λ ~ **404.0 nm**: 2s2 2p 4f ^3G - 2s2 2p 3d ^3F

- A wider spectral range (340 nm < λ < 430 nm) would also facilitate an N III and N IV line ratio analysis

N II term resolved line intensities

- A new N^{1+} ADF04 file with a more recent set of R-Matrix EIE rate coefficients (4d and 4f shell transitions supplemented by ADAS DW calculations) has been generated for this analysis
- PECs calculated with the new ADF04 file show a significant decrease in both 399.5 nm and 402.5 nm term resolved intensities in comparison to the ADAS 96 data
- Recombination does not contribute to 399.5 nm line, but has modest contribution to both 404.0 and 402.5 nm lines

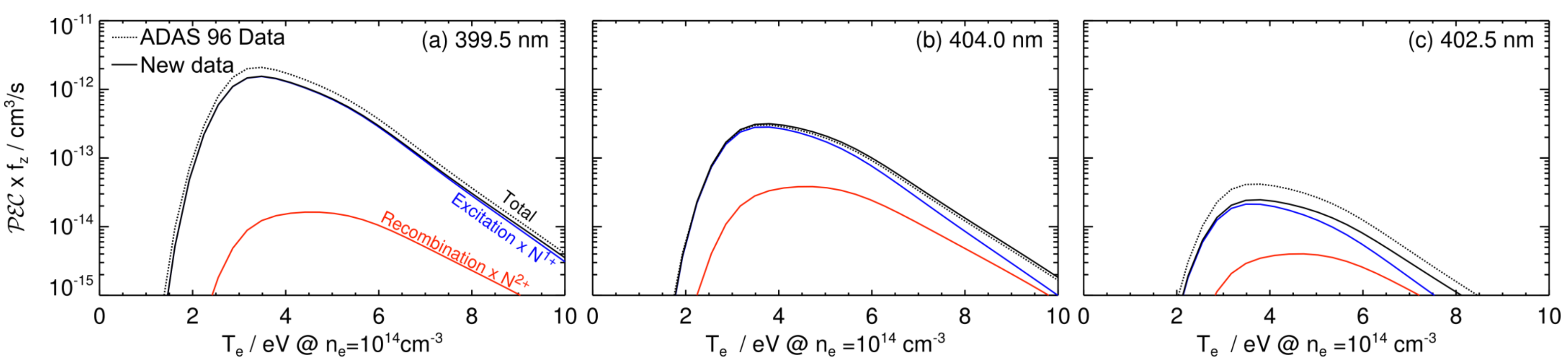

Figure 6: ADAS 96 data calculated using collision strengths from Stafford et al. *Mon. Not. R. Astr. Soc.* **268**, 816 (1994) & R. Frost, unpublished R-Matrix (1995). New data includes collision strengths from Tayal *ApJS* **195**, 12 (2011) & A. Giunta, unpublished DW (2014).

N II term resolved line ratios

- 404/399 line ratio can be used to constrain the **temperature** (for a given density)
- 404/402 line ratio provides a measure of the **density** (for $n_e > 5 \times 10^{13}$ cm^{-3})
- Self consistent pair of measured ratios is expected for localised N II emission in PFR

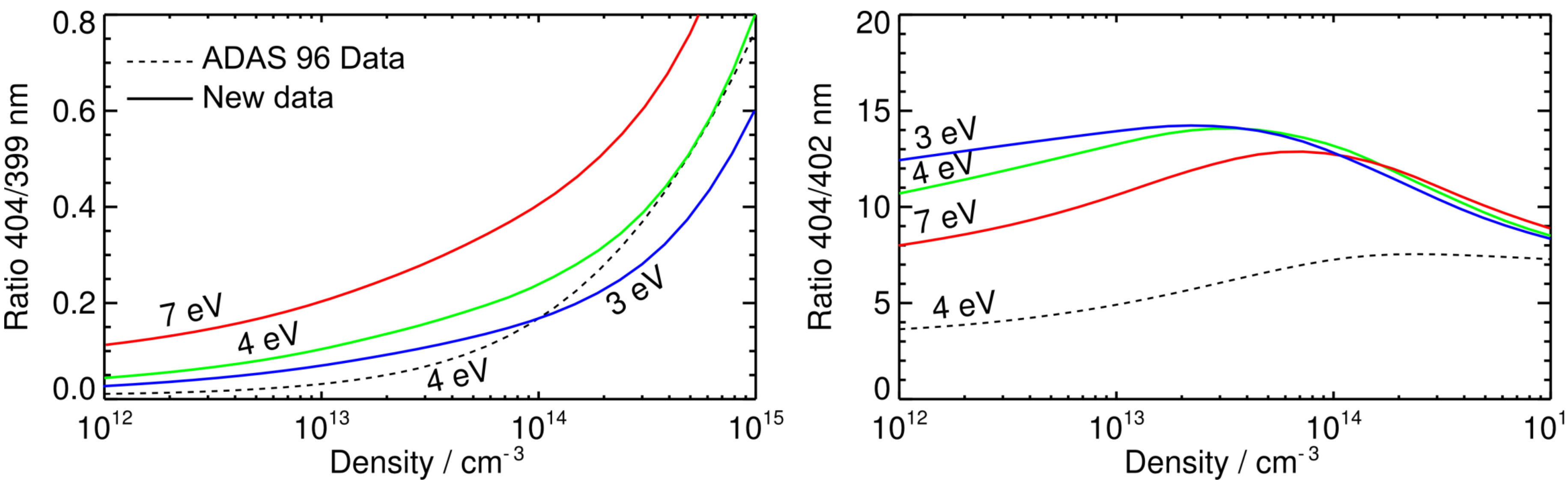

Figure 7: ADAS 96 data calculated using collision strengths from Stafford et al. *Mon. Not. R. Astr. Soc.* **268**, 816 (1994) & R. Frost, unpublished R-Matrix (1995). New data includes collision strengths from Tayal *ApJS* **195**, 12 (2011) & A. Giunta, unpublished DW (2014).

ADAS Feature Generator (AFG)

- ADAS code split_multiplet returns the relative intensity of lines in an LS multiplet
  – reasonable for line identification, but not always accurate for feature generation
- Level resolved intermediate coupling (IC) calculations available in ADAS
  – no difference between N II IC and LS intensities, but accurate for feature generation

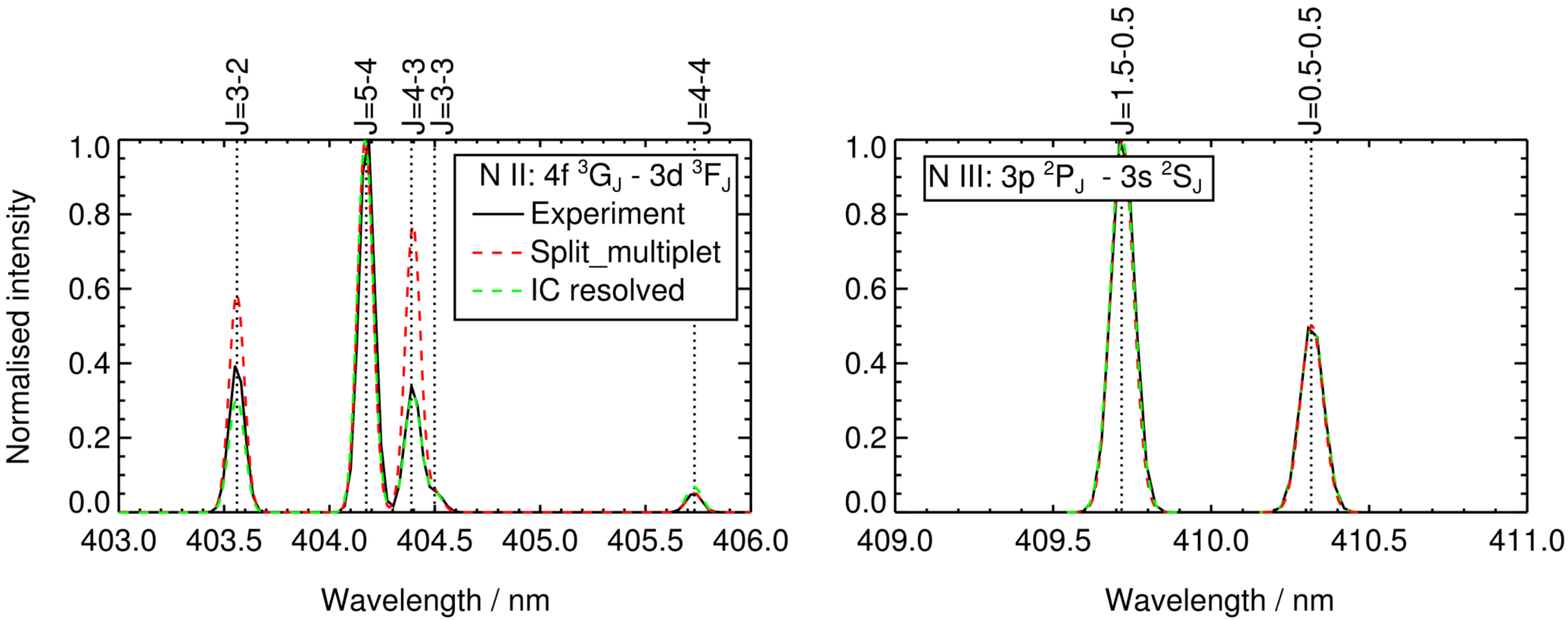

Figure 8: Experimental values represent the fitted Gaussian lines from AUG #33285. Split_multiplet is based on an algorithm by Condon and Shortley (Chap 9, Sec. 2, Eqn. 2a and 2b).

Framework for Feature Synthesis (FFS)

- Model of spectra includes N II AFG coupled with Gaussian & Voigtian line shapes, and the background continuum
- Least squares approach using the FFS provides fitted T_e, n_e and line integrated N^{1+} concentrations

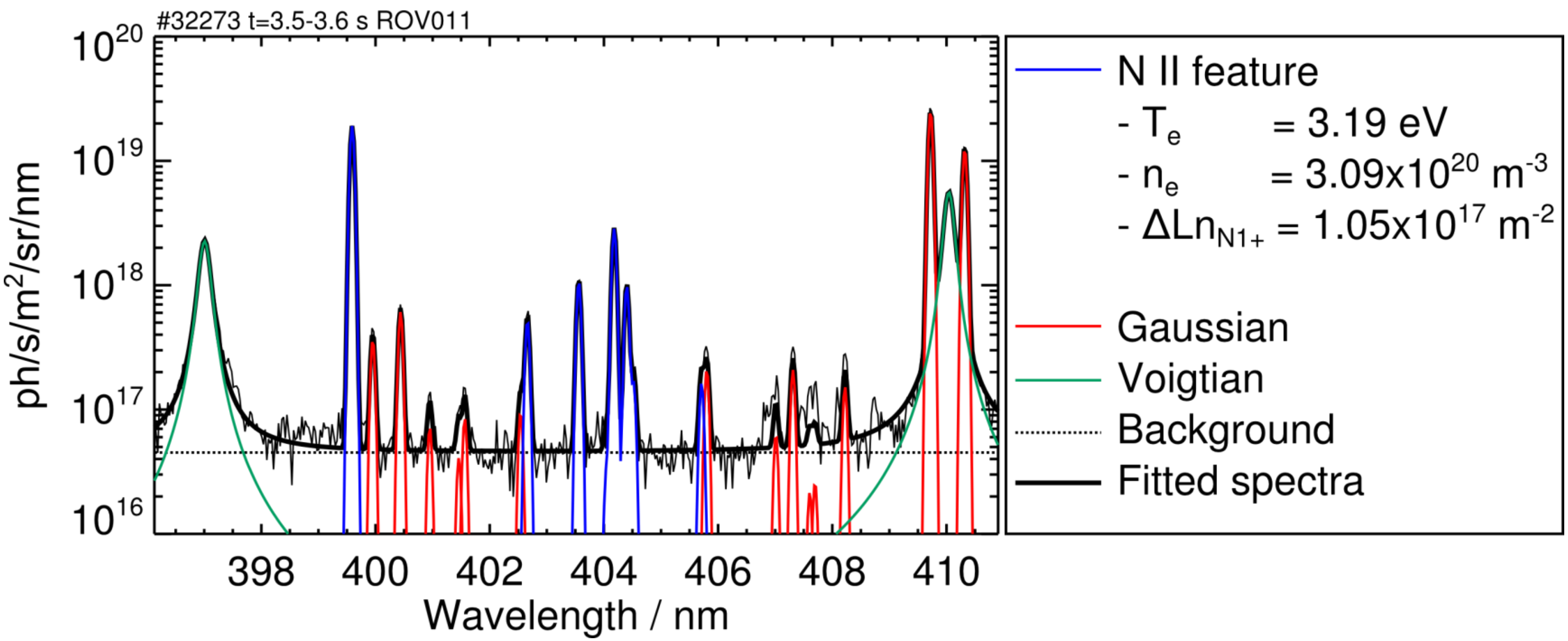

Figure 9: Model file for FFS fit includes AFG feature for N II, a multi-Gaussian parameterisation for other impurity lines, and a Voigtian parameterisation for both Balmer lines.

Framework for Feature Synthesis (FFS)

Good agreement between fitted and simulated T_e and n_e

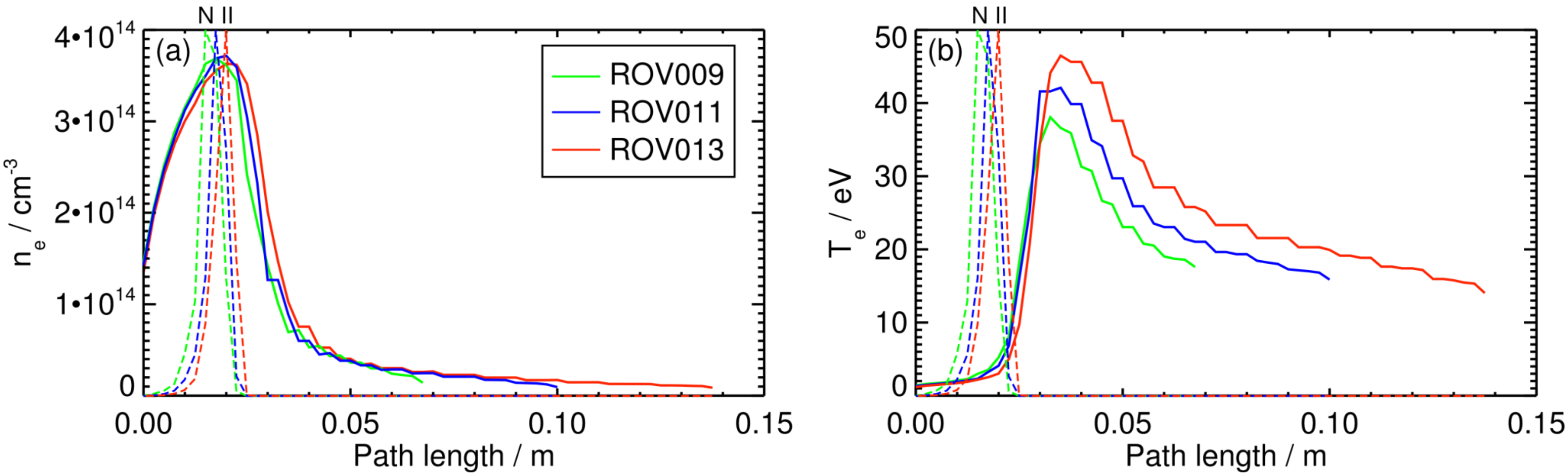

Figure 5: Sightline profiles of (a) n_e and (b) T_e as a function of the path length. Normalised N II emission is shown by the dashed lines to indicate the emitting regions.

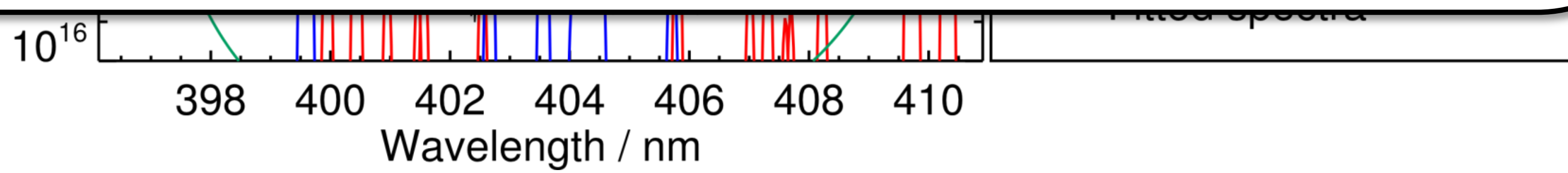

Figure 9: Model file for FFS fit includes AFG feature for N II, a multi-Gaussian parameterisation for other impurity lines, and a Voigtian parameterisation for both Balmer lines.

Temporal behaviour of fitted parameters

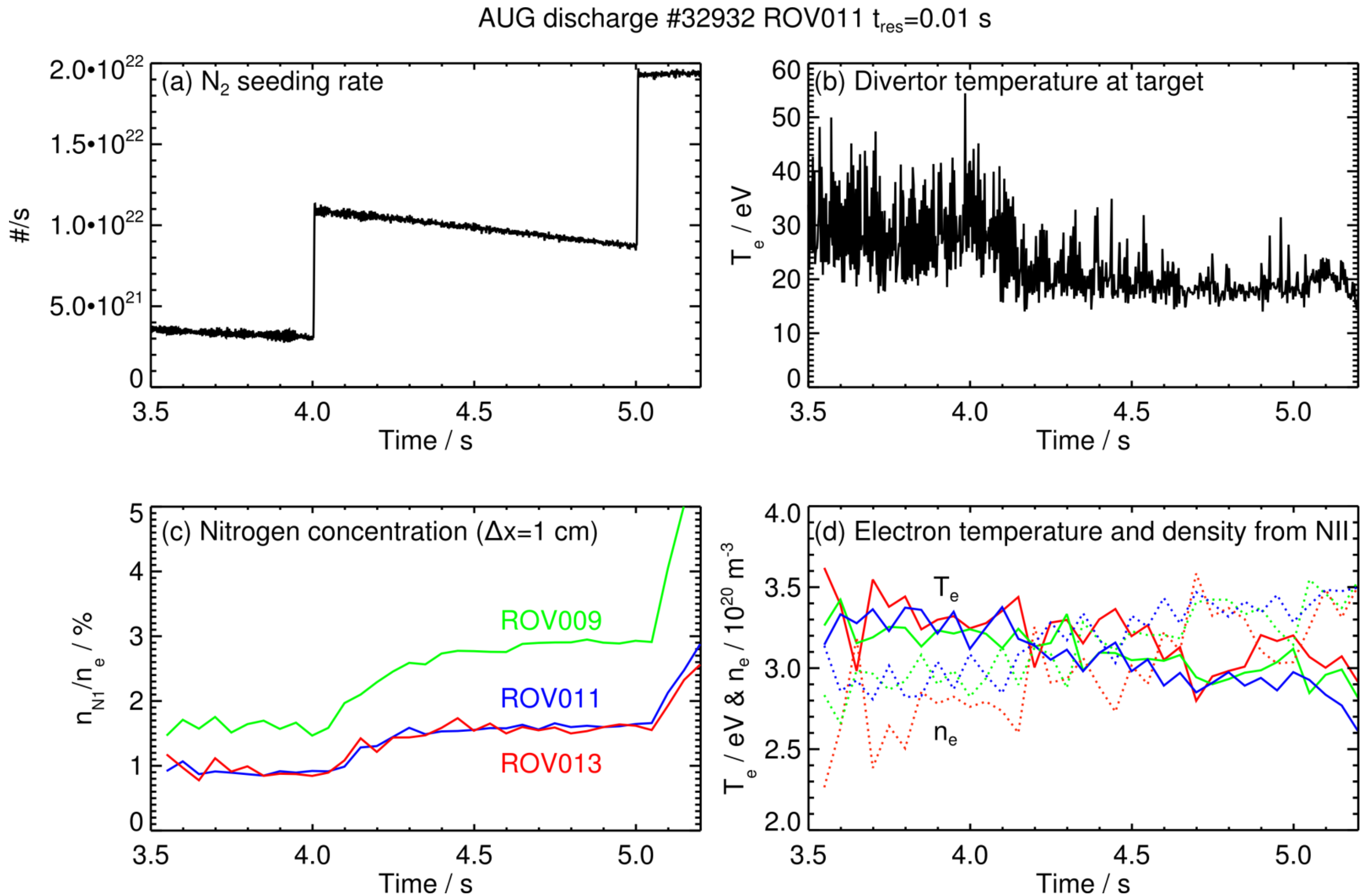

Figure 10: Fitted parameters for #32932. Time resolution has been increased to average over ELM periods. Further analysis should only model inter-ELM period (see appendix).

Summary

1) Narrow spectral range used for H_δ and H_ε Stark broadening measurements also provides a number of impurity lines useful for analysis

2) SOLPS simulations for AUG suggest that N II (and N III & N IV) emission is localised to PFR during attached divertor conditions

3) Atomic modelling of two line ratios (from three N II lines) provides a measure of the electron density and temperature, and therefore also the line-integrated N^{1+} concentration

4) Absolute values of fitted parameters agree well with SOLPS predictions in the PFR, while the temporal behaviour of fitted parameters respond accordingly to changes in N_2 seeding rate and temperature at the divertor target

Thanks for listening, any questions?

Appendix

Distinguishing between ELM and inter-ELM

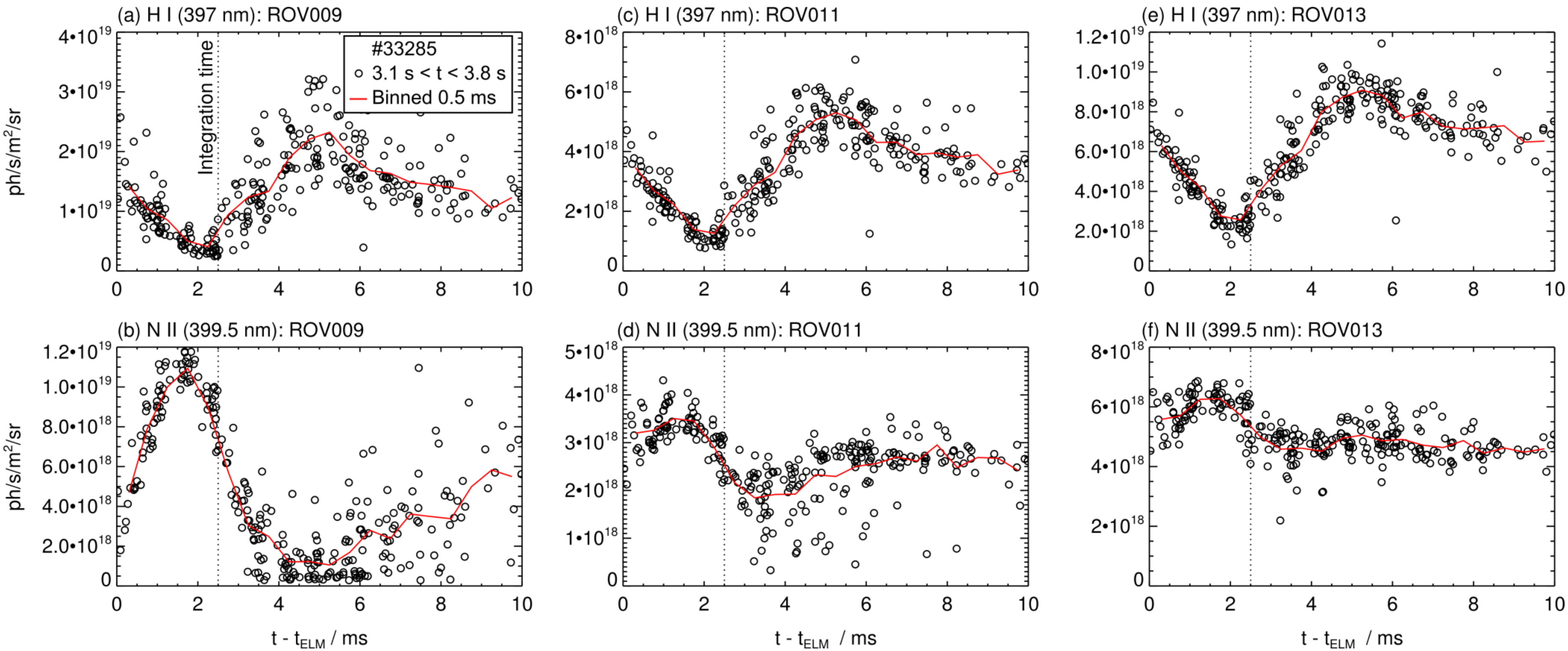

- Region of hot plasma during the ELM period ($t\text{-}t_{ELM}$=0 – 2 ms)
- Plasma cools between $t\text{-}t_{ELM}$=2 – 5 ms
- Plasma relaxes back to initial condition ~ 5 – 10 ms after ELM
- N II emission closer to target (ROV009) most sensitive to ELMs